Int J Thermophys (2012) 33:986–991
DOI 10.1007/s10765-012-1216-y

Molecular Dynamics Study of Thermal Rectification in Graphene Nanoribbons

Jiuning Hu · Xiulin Ruan · Yong P. Chen

Received: 26 June 2009 / Accepted: 11 May 2012 / Published online: 3 June 2012

Abstract Classical molecular dynamics based on the Brenner potential and Nosé–Hoover thermostat has been used to study the thermal conductivity and thermal rectification (TR) of graphene nanoribbons. An appreciable TR effect in triangular and trapezoidal nanoribbons was found. The TR factor is over 20 % even for 23 nm long monolayer triangular nanoribbons. The TR in graphene nanoribbons may enable novel nanoscale heat management and information processing using phonons.

Keywords Graphene nanoribbons · Molecular dynamics · Thermal conductivity · Thermal rectification

1 Introduction

Graphene, an atomic monolayer of graphite in the ab-plane with sp^2 carbon–carbon bonding and a honeycomb lattice structure, has received tremendous attention since its first experimental isolation in 2004 [1]. Graphene exhibits unusual electronic properties, such as massless Dirac fermions and the anomalous quantum Hall effect [2]. In

J. Hu (✉)
School of Electrical and Computer Engineering and Birck Nanotechnology Center, Purdue University, West Lafayette, IN 47907, USA
e-mail: hu49@purdue.edu

X. Ruan
School of Mechanical Engineering and Birck Nanotechnology Center, Purdue University, West Lafayette, IN 47907, USA

Y. P. Chen
Department of Physics, School of Electrical and Computer Engineering and Birck Nanotechnology Center, Purdue University, West Lafayette, IN 47907, USA
e-mail: yongchen@purdue.edu

addition, graphene shows unique thermal and mechanical properties. It has been experimentally demonstrated that graphene has a very high thermal conductivity of (3000 to 5000) $\mathrm{W \cdot m^{-1} \cdot K^{-1}}$ [3,4], among materials with the highest thermal conductivities, such as diamond and carbon nanotubes (CNTs). The strong covalent carbon–carbon bonding in graphene contributes dominantly to the thermal conduction, whereas the contribution from the electrons is negligible [4] at typical experimental temperatures. This covalent bond also makes graphene one of the strongest materials in the world [5]. Due to those properties, graphene is considered as one of the most versatile materials for future nanoelectronics. Many important devices made from graphene are composed of graphene nanoribbons (GNRs), which are narrow graphene strips of few or tens of nanometers in size. As the fundamental elements in graphene-based nanoelectronics, many properties of GNRs can be tuned by their size and edge chirality. For example, both theoretical calculation [6] and experimental demonstration [7] showed that the energy gap of GNRs depends on their width. The thermal properties of GNRs are also of great interest for fundamental physics and potential applications. Recent theoretical studies showed that the thermal conductivity of GNRs depends on their edge chiralities [8,9]. The effect of thermal rectification (TR), in which the thermal conductivity in one direction is different from that in the opposite direction, is shown in asymmetric GNRs of triangular shape [8,10]. The chirality dependence of thermal conductivity and TR of asymmetric GNRs may by applied in future nanoscale energy conversion and harvesting devices or in phonon-based logic and computational devices [11–14].

In this study, we used classical molecular dynamics (MD) to study the TR of trapezoid-shaped GNRs and triangle-shaped GNRs in single- or double-layer graphene. We also calculated the size dependence of the TR of GNRs.

2 Simulation Method: Classical Molecular Dynamics

We have used classical MD based on the Brenner potential [15] to study thermal transport in GNRs. The Brenner potential is widely used in hydrocarbon systems. The anharmonic terms of the inter-carbon interaction, essential to nonlinear thermal effects such as finite thermal conductivity and TR, is automatically embedded in the Brenner potential. The typical GNRs we used in this study are shown in Fig. 1. The atoms denoted by left-pointing and right-pointing triangles at two ends of the GNRs are put in the Nosé–Hoover thermostats [16,17] at different temperatures T_{L} and T_{R} (the average temperature is $T = (T_{\mathrm{L}} + T_{\mathrm{R}})/2$). The equations of motion for the atoms in the Nosé–Hoover thermostats are

$$\frac{\mathrm{d}}{\mathrm{d}t} p_i = F_i - \gamma p_i, \frac{\mathrm{d}}{\mathrm{d}t}\gamma = \frac{1}{\tau^2}\left[\frac{T(t)}{T_0} - 1\right], \quad T(t) = \frac{2}{3Nk_{\mathrm{B}}} \sum_i \frac{p_i^2}{2m} \tag{1}$$

where the subscript i runs over all the atoms in the thermostat, p_i is the momentum of the ith atom, F_i is the total force acting on the ith atom, γ and τ are the dynamic parameter and relaxation time of the thermostat, $T(t)$ is the instant temperature of the thermostat at time t, $T_0 (= T_{\mathrm{L}}$ or $T_{\mathrm{R}})$ is the set temperature of the thermostat, N is the

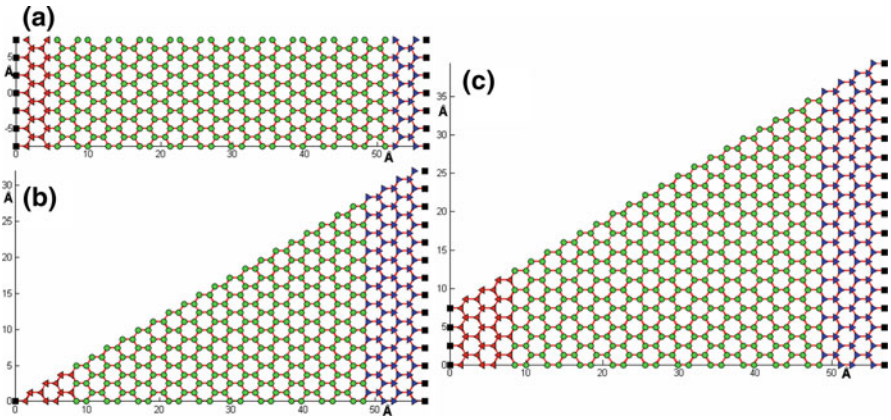

Fig. 1 Structures of GNRs in this study: (a) *rectangle*, (b) *triangle*, and (c) *trapezoid*

number of atoms in the thermostat, k_B is the Boltzmann constant, and m is the mass of the carbon atom. The atoms denoted by circles obey Newton's law of motion:

$$\frac{d}{dt} p_j = F_j, \tag{2}$$

where j runs over all the atoms denoted by circles. The atoms denoted by squares are fixed to avoid the spurious global rotation of GNRs [18]. The temperature difference at the two ends of the GNRs creates a temperature gradient and a corresponding thermal current along the temperature gradient. According to Fourier's law, the thermal conductivity can be calculated from the temperature gradient, thermal current, and size of the GNRs. In all of the following simulations, the temperature has been corrected according to the Debye model by considering the phonon occupation number. The details of the MD simulation including the quantum correction of temperature can be found elsewhere [8].

3 Thermal Rectification in GNRs

For the asymmetric GNRs (e.g., triangular and trapezoidal GNRs), the thermal conductivity from the narrower (N) to the wider (W) end and from the wider to the narrower end are denoted by $\kappa_{N\to W}$ and $\kappa_{W\to N}$, respectively. The TR factor is defined as $\eta = (\kappa_{N\to W} - \kappa_{W\to N})/\kappa_{W\to N}$. In this article, we discuss the TR of double-layer triangular and monolayer trapezoidal GNRs and compare the results with the case for monolayer triangular GNRs that we studied previously [8]. We also studied the size dependence of the TR factor for the monolayer triangular GNR as shown in Fig. 1b. The simulation results for double-layer triangular and monolayer trapezoidal GNRs are shown in Fig. 2. The double-layer triangular GNR consists of two AB-stacked monolayer triangular GNRs as shown in Fig. 1b. Compared with the monolayer triangle GNR (solid lines) of the same size, the double-layer triangle GNR (dashed line) has a larger thermal conductivity. The enhanced thermal conductivity of the double-layer GNR probably comes from the interlayer interaction which can generate several new

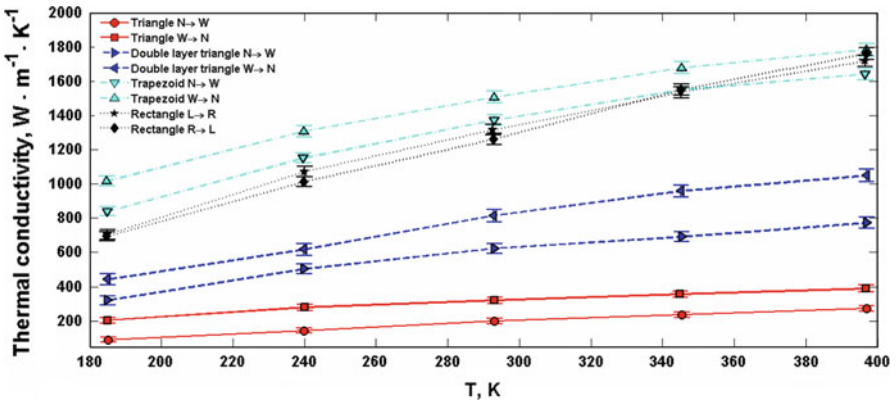

Fig. 2 TR of GNRs. The shape and size of the GNRs are specified in Fig. 1

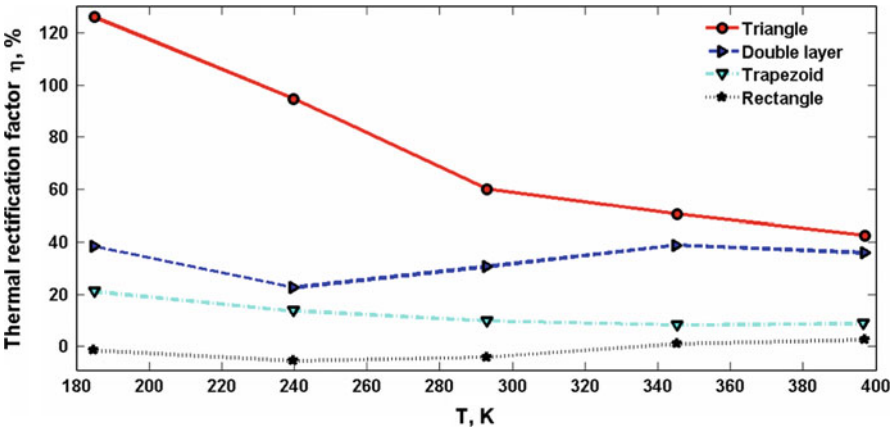

Fig. 3 Thermal rectification factor

phonon modes, such as the out-of-plane motion of those two layers that are 180° out of phase and the in-plane motion of atoms in two layers moving 180° out of phase, corresponding to the new optical dispersion branches of phonons. Those new phonon modes can contribute to the thermal conduction and thus increase the thermal conductivity. The trapezoidal GNRs (Fig. 1c, dashed-dotted lines in Fig. 2) have higher thermal conductivities than triangular GNRs (Fig. 1b, solid lines in Fig. 2), possibly due to a combination of the geometry and size dependence of the thermal conductivity [8]. For the symmetric rectangular GNR of Fig. 1a, the thermal conductivity from the left (L) to the right (R) end is almost the same as that from the right to the left end, as shown by the dotted lines of Fig. 2 (The small difference is probably from the numerical uncertainty and fluctuations related to MD simulation). The temperature dependence of the thermal conductivity of the rectangular or trapezoidal GNRs is found to be similar to that of the rectangular GNRs.

In Fig. 3, the TR factor as a function of temperature is calculated from the corresponding pair of lines in Fig. 2. For the symmetric rectangular GNR, the TR factor is

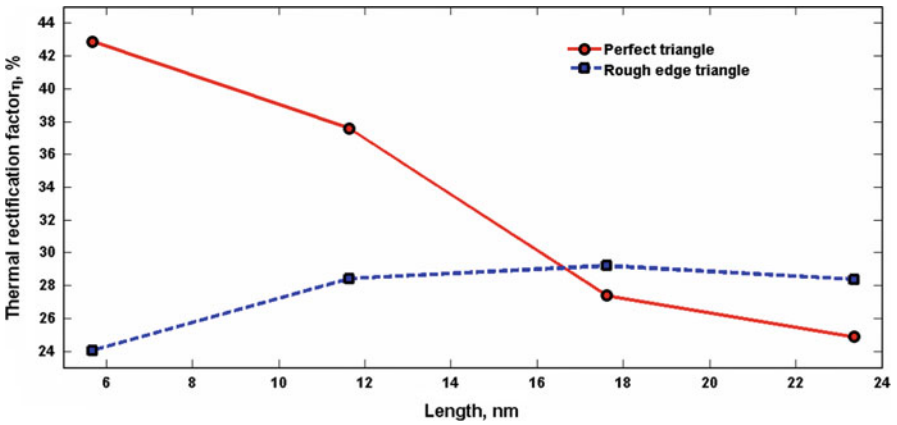

Fig. 4 Size dependence of TR factor for perfect and roughed edge triangular GNRs

consistent with zero within the MD uncertainty. For the other asymmetric GNRs, the TR factor is always larger than zero and reaches as high as 120 % for the monolayer triangular GNR at $T = 180$ K. The monolayer triangular (solid line) GNR has a larger TR factor than the double-layer triangular GNR, which has yet a larger TR factor than the trapezoidal GNR.

In Fig. 4, we show the size dependence of the TR factor for a monolayer triangular GNR in Fig. 1b with perfect (solid line) and rough (dashed line) edges. The atoms at the bottom and hypotenuse edges of various sized triangular GNRs are removed with a constant line density of about one vacancy per 1.5 nm to create edge roughness. The TR factor of perfect triangular GNRs decreases with an increase of the size, but is still as large as 25 % for GNRs of up to 23 nm long. The size dependence of the TR factor of rough-edged triangular (dashed line in Fig. 4b) GNRs shows a different behavior from that of perfect GNRs, but it appears that the TR factor converges to around 30 % as we increase the size of both the perfect and rough-edge triangular GNRs.

4 Conclusions

In summary, we have studied the thermal transport properties of GNRs using classical MD simulation. The asymmetric triangular and trapezoidal GNRs show a considerable TR effect, and the size dependence of the TR factor of the monolayer triangular GNR indicates that the TR factor is still as large as (20 to 30)% for a 23 nm long triangular GNR even in the presence of edge roughness.

Acknowledgments This study was supported by the Semiconductor Research Corporation (SRC)—Nanoelectronics Research Initiative (NRI) via Midwest Institute for Nanoelectronics Discovery (MIND). We thank Dr. Gang Wu (National University of Singapore) for helpful communications on the MD code and Mr. Yaohua Tan (Purdue University) and Prof. Zhigang Jiang (Georgia Tech) for insightful discussions on graphene.

References

1. K.S. Novoselov, A.K. Geim, S.V. Morozov, D. Jiang, Y. Zhang, S.V. Dubonos, I.V. Gregorieva, A.A. Firsov, Science **306**, 666 (2004)
2. A.H. Castro Neto, F. Guinea, N.M.R. Peres, K.S. Novoselov, A.K. Geim, Rev. Mod. Phys. **81**, 109 (2009)
3. A.A. Balandin, S. Ghosh, W. Bao, I. Calizo, D. Teweldebrhan, F. Miao, C.N. Lau, Nano Lett. **8**, 902 (2008)
4. S. Ghosh, I. Calizo, D. Teweldebrhan, E.P. Pokatilov, D.L. Nika, A.A. Balandin, W. Bao, F. Miao, C.N. Lau, Appl. Phys. Lett. **92**, 151911 (2008)
5. C. Lee, X. Wei, J.W. Kysar, J. Hone, Science **321**, 385 (2008)
6. Y.W. Son, M.L. Cohen, S.G. Louie, Nature **444**, 347 (2006)
7. M.Y. Han, B. Özyilmaz, Y. Zhang, P. Kim, Phys. Rev. Lett. **98**, 206805 (2007)
8. J. Hu, X. Ruan, Y.P. Chen, Nano Lett. **9**, 2730 (2009)
9. J. Jiang, J. Wang, B. Li, Phys. Rev. B **79**, 205418 (2009)
10. N. Yang, G. Zhang, B. Li, Appl. Phys. Lett. **95**, 033107 (2009)
11. B. Li, L. Wang, G. Casati, Phys. Rev. Lett. **93**, 184301 (2004)
12. B. Li, L. Wang, G. Casati, Appl. Phys. Lett. **88**, 143501 (2006)
13. L. Wang, B. Li, Phys. Rev. Lett. **99**, 177208 (2007)
14. L. Wang, B. Li, Phys. Rev. Lett. **101**, 267203 (2008)
15. D.W. Brenner, Phys. Rev. B **42**, 9458 (1990)
16. S.J. Nosé, Chem. Phys. **81**, 511 (1984)
17. W.G. Hoover, Phys. Rev. A **31**, 1695 (1985)
18. P.H. Hunenberger, Adv. Polym. Sci. **173**, 105 (2005)